Viruses as a tool in nanotechnology and target for conjugated polymers

Gruszka, Agnieszka

Chapter 5 Interactions of amphiphilic polyfluorenes with model membranes

5.1 Introduction

Biological membranes play an essential role in any form of life. They do not only separate the cell interior from the surrounding environment but also mediate a variety of biologically important processes. The cellular membrane composition is very complex and cannot be simply averaged over the surface. It is a lipid and protein assembly that is dynamic in nature and it simultaneously facilitates multiple, topologically distant events[1]. The most frequent processes in biology, e.g. membrane fusion, are solely dependent on the lipid bilayers[2,3]. It can be said that any interaction of a molecule with the cellular membrane can have significant consequences on its barrier function and on any of the processes that it mediates. Therefore, cellular membranes have remained in the focus of researchers since decades.

In general, to avoid overwhelming complexity of biological processes, model systems are employed in membrane research. Hence, for in vitro studies biomembranes are reconstituted from their lipid components, either natural- (Figure 5.1) or (semi)synthetic ones, which self-assemble into layered structures.

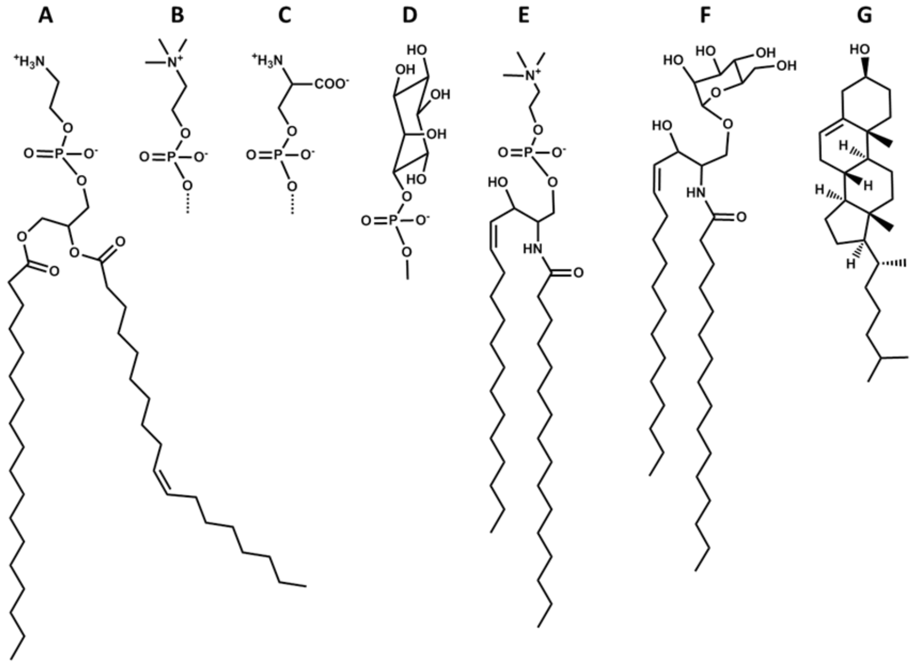

Figure 5.1. Lipids governing fundamental structure of the mammalian membranes. Phospholipids (A-E) are built of two fatty acid chains attached to a phosphorylated alcohol via either glycerol molecule (phosphoglicerides A-D) or sphingosine (sphingomyielin, E); Phosphorylated alcohol groups, which are the most common in phospholipids, are derivatives of ethanolamine (A), choline (B) serine (C) or inositol (D). Glycolipids (celerbroside, F) are derived from sphingosine and contain one or more sugar units. Cholesterol (G) is also a major constituent of animal biomembranes that influences the fluidity.

Several phospholipid-based models were developed to study membrane biophysics and the mechanisms of membrane-dependent biological processes (Figure 5.2).

One of the well-established models is the supported lipid bilayer (SLB). SLBs are defined, homogenous and a planar imitation of biological membranes. They are created with the help of Langmuir-Blodgett technique or by fusion of small lipid vesicles with hydrophilic substrates. SLBs are spread on smooth solid surfaces such as glass, gold, silicon, mica or even a polymer film[4,5].

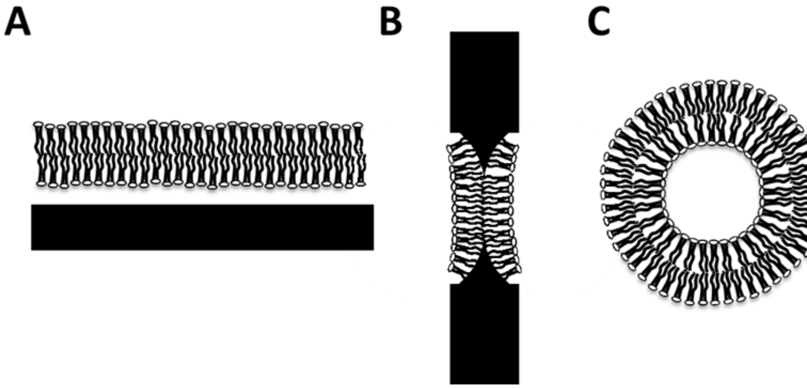

Figure 5.2. Schematic representation of model lipid bilayers: (A) Supported Lipid Bilayer, (B) Black Lipid Membrane, and (C) Liposome.

The main advantage of SLBs over un-supported models is that their surface can be analysed with several powerful techniques like atomic force microscopy, the quartz crystal microbalance, surface plasmon resonance and fluorescence microscopy[4]. The potential of SLBs as a model system is however limited to the investigations of interactions of the lipid head groups from outer leaflet since the other side is involved in supporting and therefore access to it is hindered[6].

The so called Black Lipid Membrane (BLM) was the first lipid bilayer model[7]. It is a membrane painted on a small aperture, which is separating two chambers with aqueous solution. Ever since transmembrane proteins were successfully incorporated in BLMs, this technique and its variant, the patch clamp method, became very popular in electrophysiology. With a simple electric characterization set-up, ion channels and transmembrane transport phenomena can be investigated[8,9].

Another well established membrane model system is the liposome[10]. Liposomes are spherical closed lipid bilayer assemblies with an internal aqueous compartment. They are formed upon hydration of a lipid film. These vesicles can be prepared in wide size range depending on the intended study. High energy sonication aids formation of small unilammelar vesicles (≤50 nm, SUVs), which are the most unstable ones due to the high curvature. Uniformly sized large vesicles (LUVs, 50-200 nm) are prepared by multiple extrusion steps through a porous membrane. The giant ones (GUVs, up to 100 µm) come close to the actual size of a cell and are currently prepared by electroformation. GUVs are observable with optical microscopy and can be used to study processes at the single vesicle level. All sizes of liposomes are very useful in studying different aspects of fundamental biological processes.[11]

Liposomes (mainly LUVs) have been widely applied in pharmacology as drug delivery system and to study permeability characteristics of drugs. Many of the currently used medications have an intracellular target and therefore need to cross the membrane to reach their site of action. The chance of any drug to penetrate the membrane and enter the cell is defined by its partition-coefficient (logP). This represents an important parameter influencing the efficacy of a drug. The logP is conventionally determined in a water:octane mixture and therefore often doesn't match pharmacological reality, where the membrane lipids are the hydrophobic phase[12]. For that reason liposomal membranes were employed to model and thoroughly investigate interactions of several anticancer drugs e.g. paclitaxel, gemcitabine, daunomicin or cisplatin and their derivatives with cancer cells. Those studies answered many questions and brought up the conclusion that any insight of how anticancer compounds and their carriers interact with physiological and pathological cellular membranes highly aids advanced drug design[12] .

Liposomes were also found to be a good model to study interactions of anti-infectives with membranes. Rifabutin is a broad spectrum antibiotic exhibiting high tropism to lipid membranes of infected cells and bacteria but at the same time exhibits low cytotoxicity. The experiments performed with mammalian- and bacterial-cell mimicking liposomes revealed that Rifabutin causes perturbations in the model bacterial membranes while being practically inert to mammalian cellular lipids. These results were in good agreement with in-vivo observations[13]. Another example is Oritavancin. This drug belongs to the lipoglycopeptides, a new class of antibiotics, that is based on Vancomycin's scaffold and synthesized to overcome wide spread antibiotic resistance. Vancomycin inhibits cell wall synthesis in gram-positive bacteria and therefore its derivatives are expected to act in a similar manner. However, Oritavancin that carries a lipophilic moiety was found to destabilize model membranes in a surfactant-like way. Therefore, a novel mechanism of action of this drug was demonstrated[14]. There are many examples of molecules for which activity was rationalized in studies with model membranes. Although the research in this field has been so far retrospective, it can certainly become a powerful predictive tool to develop new drugs and their delivery systems[14].

One of numerous membrane-mediated cellular processes is viral infection, which results in the fusion of a virion and a cell. Here, liposomes have turned out to be a good candidate to study early stages of viral entry. Already 30 years ago the “infection” of receptor-decorated liposomes with influenza viruses was imaged[15]. Moreover permeabilization of model bilayers by exposure to entire virions as well as to viral peptides and proteins was described and quantified by employing phospholipid vesicles[16]. In another study, the interaction between a virus and a liposome-anchored receptor was used to mimic and analyse viral docking to host cells[17,18].

Although it is known that the virus entry is mainly activated by a variety of virus/host dependent factors[19,20], it can be largely affected by the change of membrane properties[21,22,23]. Hence, the interaction of conjugated polyelectrolytes shown in Figure 5.3 with lipid bilayers may be the key to their biological activity revealed in Chapter 4.

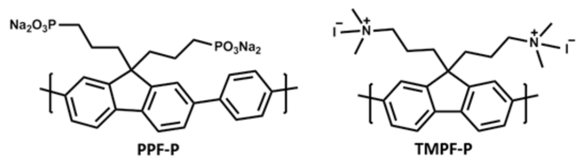

Figure 5.3. Chemical structure of amphiphilic polyfluorenes poly(9,9-bis(3’-phosphonic acid propyl)fluorene-2,7-diyl-*alt*-1,4-phenylene) (PPF-P) and cationic poly(9,9-bis(3’-(N,N,N-trimethylamino)propyl)fluorene-2,7-diyl-*alt*-1,4-phenylene) iodide (TMPF-P) used in the study.

In this chapter, we will explore the influence of charged polyfluorenes on anionic and neutral model membranes. The membrane stability will be investigated with dynamic light scattering (DLS), fluorophotometry and cryo-electron microscopy (cryo-EM). Next, the measured effects will be compared to the influence of reference polymers with known bioactivity[24,25,26].

5.2 Results and discussion

5.2.1 Vesicle design

We designed three model liposomal systems as shown in Table 5.1. Two parameters were taken into consideration: overall net charge of the membrane surface and the cholesterol content. The virion mimicking liposome resembles the Human Immunodeficiency Virus (HIV) in respect to its lipid composition[27]. Correspondingly, the cell-like vesicle composition is an approximate of the HIV host, the MT-4 cell[28]. In both cases the virion- and cell-vesicle's lipid bilayers are negatively charged. However, the virion-vesicle carries significantly more negative charges than the cell-like one and contains higher fraction of cholesterol[27]. The latter parameter is known to influence the fluidity of the bilayer. As control, neutral vesicles were included. The neutral vesicles are made purely of zwitterionic phospholipids and the cholesterol content was averaged to match mean cholesterol content in mammalian cell plasma membranes[29].

Table 5.1. Composition of model liposomes used in the experiments shown as molar ratio of all components.

	Molar ratio of lipid components*			
	DOPC	**DOPE**	**DOPG**	**Chol**
Virion vesicles	0.23	0.23	0.08	0.45
Cell vesicles	0.33	0.33	0.05	0.28
Neutral vesicles	0.33	0.33	0	0.33

** DOPG: 1,2-dioleoyl-sn-glycero-3-phosphatidylglycerol, DOPE 1,2-dioleoyl-sn-glycero-3-phosphoethanolamine, DOPC: 1,2-dioleoyl-sn-glycero-3-phosphocholine, Chol: cholesterol*

5.2.2 Dynamic Light Scattering

First, the effect of positively charged TMPF-P and negatively charged PPF-P on the model membranes was investigated with DLS. For comparison, a selection of commercially available, bioactive polymers was additionally included in this study (Figure 5.4). The majority of polyanions exhibiting antiviral activity is derived from polysaccharides. In general, they are considered to be unspecific inhibitors.

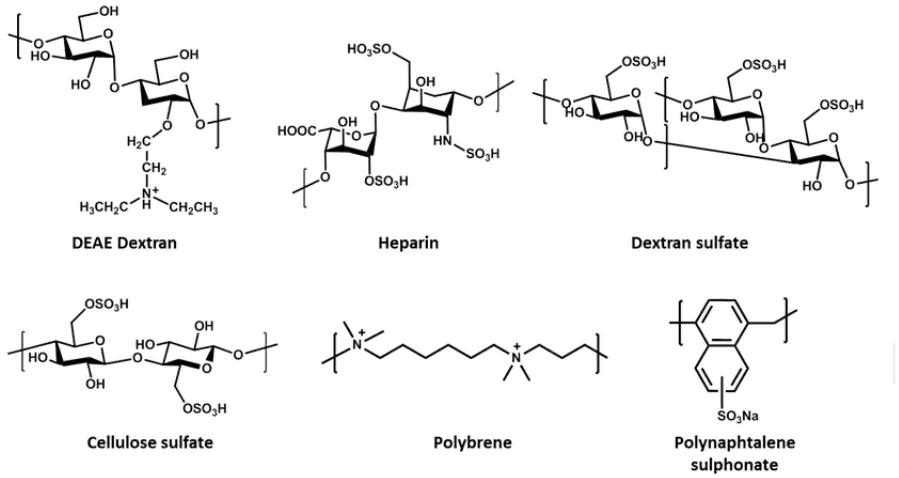

Figure 5.4. Overview of charged, commercially available polymers used in the study.

To investigate the effect of the positively charged TMPF-P and the anionic PPF-P on model membranes, they were added to a 1:1 mixture of virion and cell liposomes. Additionally, in the control experiment the polymers were incubated with neutral liposomes. The hydrodynamic radius of the vesicles was measured with DLS shortly after mixing and after 12 h of incubation at 37°C.

As shown in Figure 5.5A, untreated virion and cell vesicles maintain their narrowly distributed hydrodynamic radius of 65 nm even after 12 hour incubation. However, addition of a polyfluorene polymer to these liposomes causes a drastic change. As expected, the negatively charged vesicle pair undergoes rapid, electrostatically driven aggregation when the positively charged TMPF-P is added (Figure 5.5A). As a result, the size distribution becomes very broad and covers nearly the entire range of radii. This indicates the presence of numerous, not uniformly sized populations of liposomal aggregates in the sample.

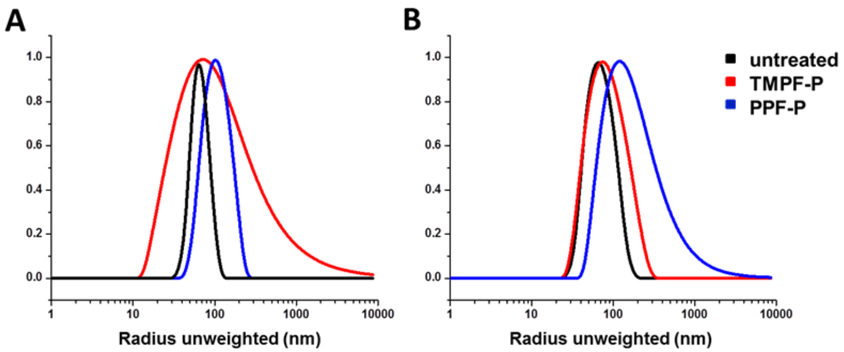

Figure 5.5. PPF-P and TMPF-P influence on model membranes measured with Dynamic Light Scattering after 12 hours of incubation with virion-cell vesicle pairs (A) and neutral vesicles (B).

The anionic PPF-P was also found to influence the virion-cell vesicles pair. Noteworthy, in this case both vesicles and polymer carry a net negative charge. After incubation the hydrodynamic radius of PPF-P treated vesicles is significantly larger than the control. If the nature of interactions between phospholipids forming the membrane and the polymer was purely electrostatic, no change would be expected due to the repulsive forces between the negatively charged species. Since the results show the opposite, other features must play an important role as well. Therefore we have additionally investigated the influence of PPF-P and TMPF-P on vesicles with zero net charge (Figure 5.5B). As can be observed, neutral liposomes were not particularly affected by the presence of TMPF-P. Only a slight size increase was detected, which proves the binding that have been reported in literature and attributed to an interaction of cationic polymer with phospholipid head groups[30]. In contrast, a significant size increase was observed when exposing the neutral vesicles to the PPF-P polymer. The effect seemed even larger as seen for the charged virion-cell liposome pair. This result confirms that this polymer interacts with phospholipid bilayers in a charge-independent manner, although most likely the electrostatic barrier still plays a substantial role.

Lastly the hydrodynamic radius of the virion-cell pair was measured upon addition of commercially available, bioactive polymers to the liposomal solutions. The results are included in Table 5.2.

Table 5.2. Hydrodynamic radius change upon incubation of model liposomes with charged polyfluorenes and reference bioactive polymers.

	Incubation time	
	5min	**12hrs**
Virion + cell vesicles	**radius nm**	
TMPF-P	150	300
PPF-P	71	106
DEAE Dextrane	64	65
Polybrene	65	66
Polynaphtalene sulphonate	65	63
Dextrane sulphate	63	66
Heparin	67	66
Cellulose sulfate	66	66
Untreated	*65*	*65*
Neutral vesicles	**radius nm**	
TMPF-P	74	74
PPF-P	100	360
Untreated	*67*	*70*

As can be seen in the results summary, the untreated control vesicles maintain their size very well over the duration of the experiment. Remarkably, the addition of the positively charged TMPF-P to the virion-cell vesicles results in a rapid increase in hydrodynamic radius within the first 5 minutes, whereas the addition of the negatively charged ones has little influence. Over the course of the incubation time the presence of TMPF-P results in a further size increase, which yields much larger aggregates than the control vesicle. These aggregates were also found to quickly sediment on the bottom of the vessel as shown in Figure 5.6. The addition of PPF-P also causes an increase in size, but to a lesser extent than for TMPF-P. In contrast, the PPF-P has a much larger effect than TMPF-P when added to neutral vesicles. Both polymers alone in the solution gave a weak scattering signal, therefore, the observed size increase cannot be associated with their scattering. Finally, it is important to note that none of the reference polymers has any effect on the measured hydrodynamic radii.

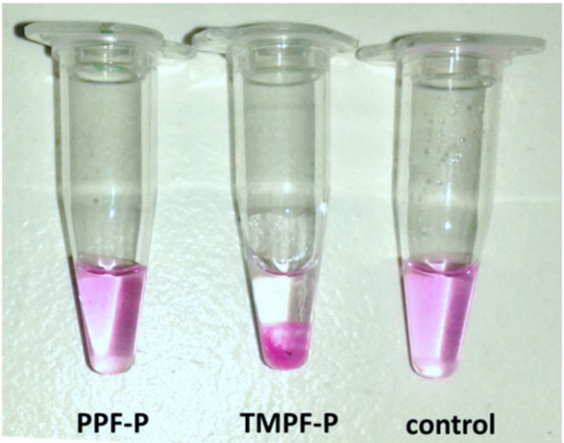

Figure 5.6. Interaction of negatively charged vesicles with different polyelectrolytes. For imaging purposes Sulforhodamine B loaded vesicles were used.

5.2.3 Membrane stability

The influence of charged polyfluorenes on the stability of the model membranes was also assessed in a fluorescence-based assay[31]. In this experiment, half of all liposomes (w/w) contained Sulforhodamine B (SB) in their lumen at a self-quenching concentration. The concentration of SB being encapsulated in the model liposomes was adjusted to give the highest signal upon 2-fold dilution. This dilution factor is expected when fusion occurs. The fluorescence intensity of the liposome solution was monitored over 6 hours of incubation under biologically relevant conditions (37°C, pH 7.4). Similar as with the previous experiment, the virion-cell and neutral liposome formulations were incubated either with PPF-P or TMPF-P and the recorded signal was compared to the untreated control sample (Figure 5.7).

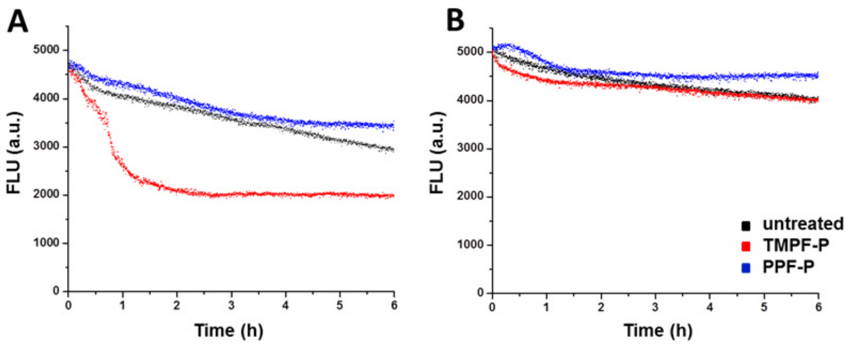

Figure 5.7. Model membranes stability in the presence of PPF-P and TMPF-P. Incubation with virion-cell vesicles (A) and neutral vesicles (B).

As shown in Figure 5.7A, TMPF-P induces a substantial change in the sample consisting of negatively charged vesicles. It causes twofold drop of fluorescence intensity already within the first hour of incubation. It must be noted here that such a drastic change in the signal is most likely caused by sedimentation of the SB containing liposomes. Hence, this result is in agreement with the rapid vesicle aggregation that is visible by the naked eye (Figure 5.6) and was previously observed with DLS (Table 5.2). Naturally, TMPF-P is expected to bind stronger to the virion vesicles as they have a higher content of anionic phospholipids (Supporting Figure 5.1). In contrast to TMPF-P, addition of anionic PPF-P results in a slightly larger SB signal compared to the control. Lastly, the fluorescence intensity in the control sample steadily decreases. This can be explained by either solvent evaporation, which causes even higher concentrations of SB, or by dye bleaching upon long-term irradiation.

The influence of PPF-P and TMPF-P on virion-cell liposomes pair is opposite but in both cases the SB fluorescence intensity reaches a plateau. However, this does not necessarily mean that the samples are equilibrated. One should correct the obtained signal by the steady decrease of the emission observed in the control sample. For PPF-P the net result of this correction is a small increase of SB fluorescence over the duration of experiment. Upon correction, the signal of TMPF-P also slightly increases after the major drop observed in the first hour. This increase must be caused by dilution of initially encapsulated, water-soluble, fluorescent dye. There are several possibilities for SB dilution, including vesicle fusion, increase of membrane permeability and membrane rupture. The latter cause can easily be simulated by addition of a commonly used surfactant, Triton-X. This results in liposome destruction, rapid dilution of the encapsulated SB and a 400-500% fluorescence increase. As such, the relatively low increase of the fluorescence indicates that the liposomes are not harmed by the presence of PPF-P. However, in the long term the integrity of lipid bilayers is affected by the polymer and the small SB molecules might leak out from liposomal lumen.

When looking at the neutral vesicles it becomes apparent that they are more influenced by the presence of the anionic polymer (Figure 5.7B). The fluorescence starts to increase already after a short time of incubation. In contrast, neutral liposomes treated with cationic TMPF-P show a minor drop in fluorescence at the beginning of the experiment, which might indicate some aggregation. However, this was not observed in the DLS experiment.

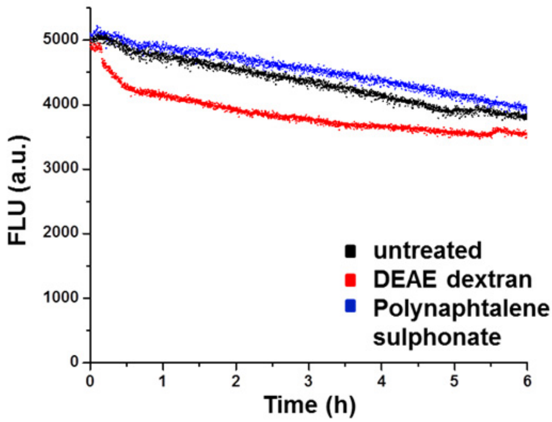

Figure 5.8. Virion-cell vesicles stability in the presence of DEAE dextran and polynaphtalene sulfonate.

Finally, the model membrane stability in the presence of commercially available antiviral polymers was investigated (Figure 5.8). Among them, DEAE dextran was found to give the largest effect and caused a 22% loss of the fluorescence intensity, after correcting for the control signal. However, no aggregation was detected with DLS for the same sample (Table 5.2). The second active molecule, the anionic polynaphtalene sulfonate did not give a significant increase of the SB emission intensity.

It must be noted that the fluorescence signal in both cases decreased in a similar manner as in the control sample.

3.2.4 Cryo-EM

To obtain more insight into the influence of TMPF-P and PPF-P on the model membranes transmission electron microscopy at cryogenic temperatures (cryo-EM) was chosen as complementary characterization technique. This method allows observation of soft matter in its native environment and is therefore very well suited to study the effects of our polyfluorenes on the liposomal formulations.

As described before, the virion-cell liposome mixture was incubated with both polyfluorenes TMPF-P and PPF-P. Upon studying the TMPF-P treated liposomes, aggregation driven by the polymer was clearly observed (Figure 5.9A). Representative micrographs show liposomal aggregates over large surface areas of several square micrometers. However, despite the clustering, the liposomes remain regularly shaped. The positively charged TMPF-P polymer alone spreads over large surfaces in solution and forms irregular sheet-like structures (Figure 5.9B). In such structures, the cationic groups are possibly exposed to the solvent to maintain solubility in the aqueous environment, while the fluorene-based backbone assembles in the core due to its hydrophobicity and π-π stacking. This flat structure possibly served as a 2D scaffold for attachment of oppositely charged liposomes, thereby, being a key factor in the observed vesicle aggregation.

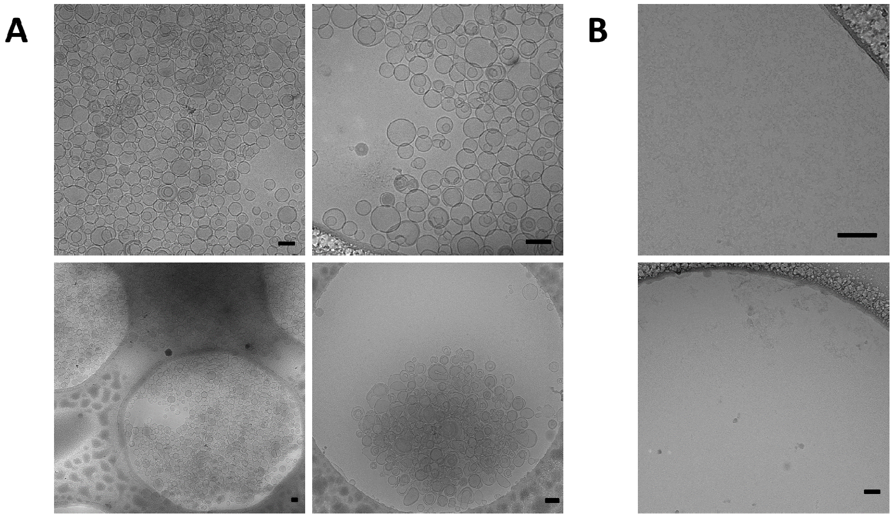

Figure 5.9. Cryo-EM micrographs of (A) the virion-cell vesicle pair treated with TMPF-P and (B) the polymer TMPF-P in solution. Scale bars are 100 nm.

Such aggregates could not be found in solution of the untreated liposomes. These vesicles were observed as regular spheres without obvious aggregation behavior (Figure 5.10).

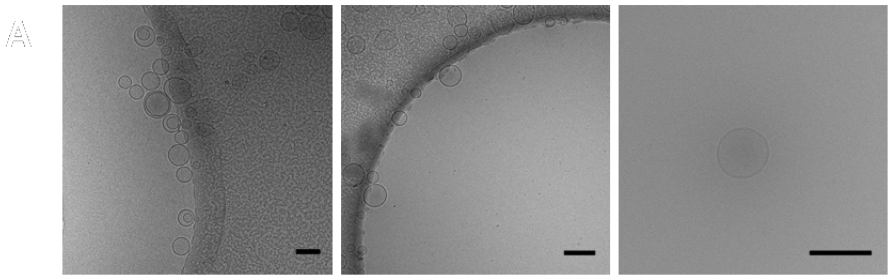

Figure 5.10. Cryo-EM micrographs of untreated virion-cell vesicle samples. Scale bars are 100 nm.

Subsequently, the anionic polymer interacting with negatively charged vesicles was imaged (Figure 5.11A). The PPF-P itself was recognized as small aggregates attached to the membranes (red arrows in Figure 5.11A). Additionally, a population of enlarged vesicles was found in the sample, which might indicate possible fusogenic activity of the negatively charged polyfluorene. Indication for a size increase especially for neutral vesicles was also observed by DLS. Similar to TMPF-P, the PPF-P also forms 2D structures when being dissolved alone in solution

(Figure 5.11B). However, these aggregates were not prone to attract liposomes presumably due to the electrostatic repulsion. The strong aggregation behavior of the polymer was additionally confirmed with fluorophotometry, where its intrinsic fluorescence was self-quenched when a concentration of 25 ug/mL was reached (Supporting Figure 5.2). This can explain why a relatively high concentration of PPF-P was necessary to fully deactivate HIV virions as presented in Chapter 4.

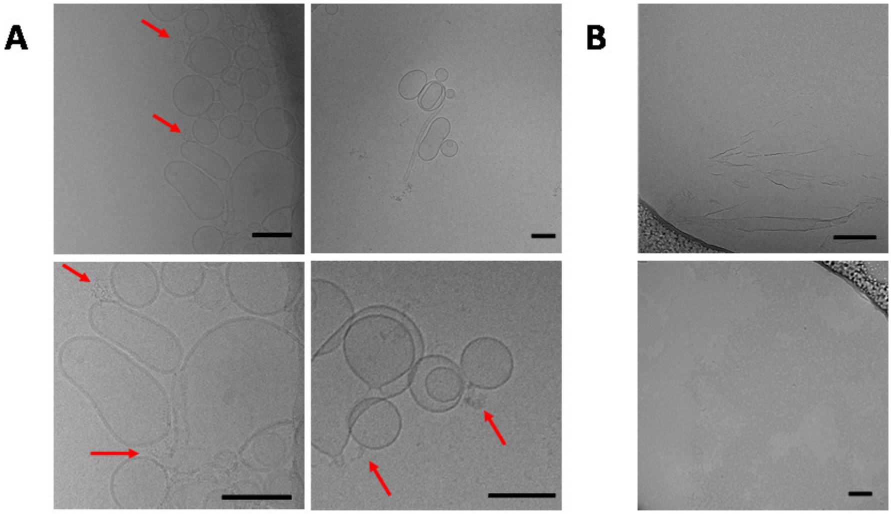

Figure 5.11. Cryo-EM micrographs of (A) the virion-cell vesicles pair treated with PPF-P and (B) the polymer PPF-P only control in solution. Scale bars are 100 nm.

Finally, the virion-cell vesicle pair was also treated with the control polymers. As shown in Figure 5.12A, in the sample of liposomes treated with polynaphtalene sulfonate some irregularities in shape were present. The liposomes treated with DEAE dextran (Figure 5.12B) showed no major differences when compared to the untreated liposomes. Noteworthy is that these are the two commercial polymers that showed the most pronounced effect in the membrane stability assay.

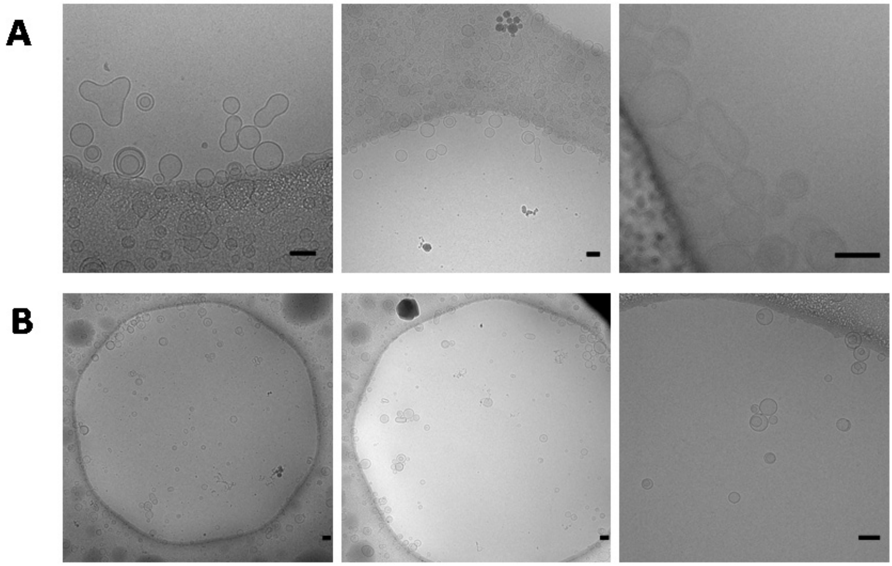

Figure 5.12. Cryo-EM micrographs of virion-cell vesicle formulation treated with commercially used polymers with an antiviral activity: (B) polynaphtalene sulfonate and (C) DEAE dextran. Only compounds with the highest activity in the membrane stability assay are presented. Scale bars are 100 nm.

5.3 Conclusions

In this chapter, the stability of model liposomes was assessed in the presence of cationic and anionic variants of polyfluorenes. A pair of negatively charged vesicles was designed to mimic a HIV virion and its host, a MT-4 cell. The two parameters taken into consideration here were their overall surface charge and the membrane fluidity, which is reflected by the cholesterol content. Additionally, neutral vesicles were employed in order to judge the influence of the electrostatic barrier.

The interactions between the liposomes and polymers were studied by DLS, a fluorescence based assay, which demonstrated the membrane stability, and cryo-EM. It was found that the TMPF-P polymer caused rapid changes in the sample and resulted in formation of a precipitate, a phenomenon that is mainly electrostatically driven. On the other hand, the negatively charged PPF-P also interacted with the membranes, but in a charge independent manner. The tested lipid bilayers were stable against both fluorene-based amphiphiles. Incorporation of PPF-P might result in weak leakage.

In previous chapter, TMPF-P was found to enhance HIV infectivity. We hypothesised that the positively charged polymer neutralized the negatively charged surface of the virions and cells, and therefore promoted the transfection. In fact, the experiments performed in this chapter supported this observation. Negatively charged liposomes strongly aggregated upon treatment with TMPF-P, which was demonstrated with all employed techniques. The aggregation was proportional to the content of anionic phospholipids in the model membranes, which further confirmed the impact of electrostatic forces on activity of the cationic polymer. Thus, we expect that TMPF-P reduced electrostatic repulsion between viruses and cells in a similar fashion. This led to virus coagulation and subsequent sedimentation, which might increase the chance of infection.

On the other hand, the polyfluorene modified with negatively charged phosphonate groups inhibited HIV infection. Previously we anticipated that the PPF-P targets virus particles because cell pre-treatment with the polymer did not influence the infection rate. Indeed, here we found a certain degree of membrane destabilization by the anionic polymer, as shown in the fluorescence based assay. What can be concluded from the experiments is that the virus membranes are not disrupted by the anionc polymer. Despite the repulsive electrostatic interaction, the polymer was found to interact with the membrane of model liposomes causing a size increase, as proved by DLS and cryo-EM. This finding is underlined by the fact that the neutrally charged membrane was in general more influenced by PPF-P. Finally, we showed that PPF-P aggregates into sheet-like structures in solution. We expect that such big aggregates were more prone to influence the activity of small viruses than the significantly larger cells. Therefore cell-treatment did not show any effect.

Regarding the anionic polymers acting as virucidal agent, one can conclude that PPF-P most probably interacts with the viral membrane. The driving force for this interaction is the hydrophobic polymer backbone inserting into the hydrophobic part of the lipid bilayer. The conjugated polymer with its negative charges might interfere with the recognition of receptors on the cell surface. In fact there are some cationic domains within viral fusion proteins which proved crucial for viral infection[32-34]. Another explanation for reducing viral activity might be that the polymer shields the whole virus and/or changes the physical properties of the virus membrane to inhibit further fusion events.

However, the investigation about the precise mode of action of PPF-P requires further experiments.

5.4 Materials and methods

Lipids 1,2-dioleoyl-sn-glycero-3-phosphatidylglycerol (DOPG), 1,2-dioleoyl-*sn*-glycero-3-phosphocholine (DOPC), 1,2-dioleoyl-*sn*-glycero-3-phosphoethanolamine (DOPE) and cholesterol (Chol) were purchased from Avanti Polar Lipids. Anhydrous chloroform was purchased from Acros Organics. Sulforhodamine B and Sephadex G-75 resin were purchased from Sigma-Aldrich. Fluorescence was measured on a SpectraMax M2 spectrophotometer (Molecular Devices, USA) using Greiner Bio-One 96-Well black microplates (VWR, The Netherlands). Dynamic Light Scattering was measured on an ALV/CGS-3 goniometer system working in autocorrelation mode and using the JDSU 1145/P HeNe laser (λ=632.8 nm). Quantifoil 3.5/1 holey carbon-coated grids (QUANTIFOIL Micro Tools GmbH) were purchased from Science Services (Germany). DEAE dextran, dextran sulfate, heparin, polynaphtalene sulfonate and cellulose sulfate were kindly provided by Prof. Dr. Jan Münch.

The synthesis of the used polyfluorenes PPF-P and TMP-F was described in Chapter 4.

Preparation of liposomes – general procedure
Liposomes, at a final concentration of 1.2 mg/mL, were prepared according to generally known procedures. Briefly, lipids (DOPC, DOPE, DOPG and cholesterol) dissolved in anhydrous chloroform were mixed in the desired molar ratio. Chloroform was evaporated with a gentle stream of nitrogen and additionally in vacuum (2 h). The dried lipid film was rehydrated in PBS buffer by vortexing with glass beads and shortly sonicated. Next, the vesicles were subjected to 10 cycles of rapid freezing in liquid nitrogen and thawing in 50°C water bath. Afterwards the liposomes were extruded 21 times through a 100 nm polycarbonate film (Avestin).

Sulforhodamine containing liposomes were prepared in the same manner except for the rehydratation step which was done in PBS buffer supplemented with 2.5 mM sulforhodamine B (SB). SB-loaded vesicles were purified from not encapsulated dye by size-exclusion chromatography (SEC) using Sephadex G-75 resin and PBS buffer as an eluent to prevent changes in osmolarity. Fractions containing SB-encapsulated liposomes were combined and total lipid concentration was determined using Stewart test, based on the measurement of absorption (λ=485 nm) of the phospholipid-ammonium ferrothiocyanate complex. SEC resulted in 2.5-fold dilution of liposomes (final concentration 0.48 mg/mL).

Model membranes stability experiment

Cell-vesicles and virion-vesicles were used in 1:1 ratio. Half of all liposomes used in the assay was loaded with sulforhodamine B. Neutral-vesicles and sulforhodamine B loaded neutral-vesicles were also mixed in 1:1 weight ratio. Samples were diluted with PBS buffer to a final volume of 196 µL, in a 96-well plate. After 5 minutes of equilibration at 37°C, polymer solution in PBS buffer was added to correspond to 8.3 weight % of total lipid concentration for cell-virion liposome pair and 13 weight % of total lipid concentration in case of neutral-vesicles pair. SB fluorescence intensity was measured over 6 hours at 37°C (λ_{ex}= 565 nm, λ_{em}=585 nm). The plate was automatically shaken before each measurement. In the control experiment same volume of PBS buffer was added to the vesicles.

Dynamic Light Scattering

Measurements were performed in a temperature controlled set up at 37°C and under a scattering angle of 90°. The average hydrodynamic radius was obtained from 3 measurements of 30 seconds each. PBS buffer used to prepare all solutions was filtered through a 0.22 µm syringe filter prior to use. The virion- and cell-liposomes were mixed in 1:1 weight ratio and diluted to obtain a final concentration of 0.075 mg/mL. Neutral vesicles were also diluted to a final concentration of 0.075 mg/mL. Solutions were equilibrated at 37°C for 5 minutes and subsequently the polymer solution was added to a final concentration of 8 weight % of the lipids or 13 weight % of the lipids in case of neutral vesicles. Hydrodynamic radii were measured 5 minutes after addition of the polymer and after 12 hours of incubation. Samples were gently shaken before the measurement.

Cryo-EM

Samples for cryo-electron microscopy were prepared by deposition of a drop (2.7 µL) of a solution on a glow-discharged holey carbon-coated grid (Quantifoil 3.5/1, QUANTIFOIL Micro Tools GmbH). Excess of solution was blotted off on a filter paper. The grid was vitrified in liquid ethane using a Vitrobot (FEI) and stored in liquid nitrogen before being transferred to a Philips CM 120 electron microscope equipped with a Gatan model 626 cryo-stage, operating at 120 kV. Images were taken in low-dose mode using a slow-scan CCD camera. The concentration of vesicles in all samples was adjusted to 1 mg/mL. In the polymer-containing vesicle samples polymer concentration was 8 weight % of the total lipid concentration. Due to technical limitations the concentration of the polymer in control samples was 1 mg/mL, which ensures quantitative imaging of the specimen.

5.5 Supporting Figures

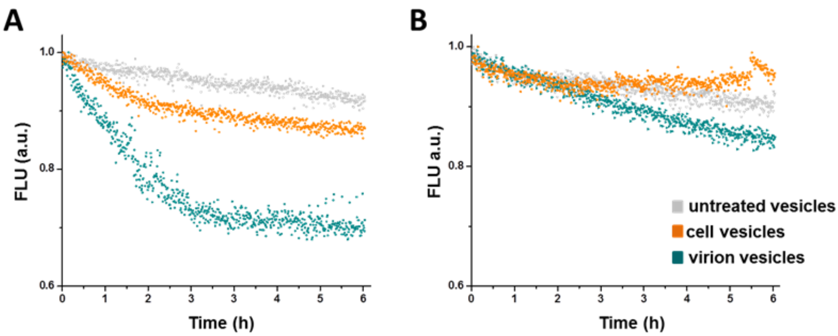

Supporting Figure 5.1. Influence of charged polyfluorenes on model membranes with different anionic phospholipid content. (A) The interaction of TMPF-P on the virion vesicles is significantly stronger than on the cell vesicles. It proves that the TMPF-P-vesicles interaction is governed mainly by electrostatic forces. (B) The membrane of cell-like liposome is more sensitive towards the anionic PPF-P. Therefore we see that also here the electrostatic barrier influences the interaction between negatively charged polymer and liposome.

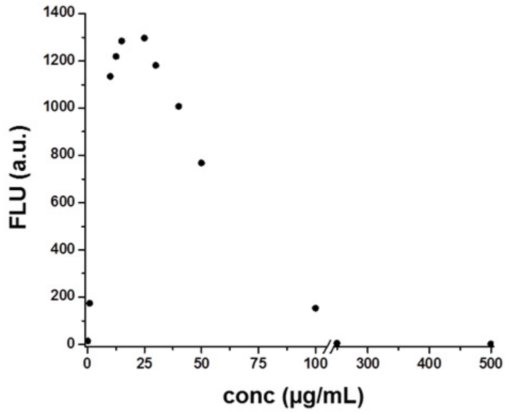

Supporting Figure 5.2. Aggregation of PPF-P in a solution was determined with measurements of the polymer fluorescence (excitation 360 nm, emission 410 nm).

5.6 Acknowledgment

I would like to acknowledge E. Warszawik for the help with polymer aggregation study and Z. Meng for help in design of the liposome studies.

5.7 References

1. Singer, S.J. & Nicolson, G.L. The fluid mosaic model of the structure of cell membranes. *Science* **175**, 720-731 (1972).
2. Jahn, R., Lang, T. & Sudhof, T.C. Membrane fusion. *Cell* **112**, 519-533 (2003).
3. Martens, S. & McMahon, H.T. Mechanisms of membrane fusion: disparate players and common principles. *Nat Rev Mol Cell Biol* **9**, 543-556 (2008).
4. Richter, R.P., Berat, R. & Brisson, A.R. Formation of solid-supported lipid bilayers: an integrated view. *Langmuir* **22**, 3497-3505 (2006).
5. Sackmann, E. & Tanaka, M. Supported membranes on soft polymer cushions: fabrication, characterization and applications. *Trends Biotechnol* **18**, 58-64 (2000).
6. Peetla, C., Stine, A. & Labhasetwar, V. Biophysical interactions with model lipid membranes: applications in drug discovery and drug delivery. *Mol Pharm* **6**, 1264-1276 (2009).
7. Mueller, P., Rudin, D.O., Tien, H.T. & Wescott, W.C. Reconstitution of cell membrane structure in vitro and its transformation into an excitable system. *Nature* **194**, 979-980 (1962).

8. Shen, H.H., Lithgow, T. & Martin, L. Reconstitution of membrane proteins into model membranes: seeking better ways to retain protein activities. *Int J Mol Sci* **14**, 1589-1607 (2013).
9. Bebarova, M. Advances in patch clamp technique: towards higher quality and quantity. *Gen Physiol Biophys* **31**, 131-140 (2012).
10. Bangham, A.D., Standish, M.M. & Watkins, J.C. Diffusion of univalent ions across the lamellae of swollen phospholipids. *J Mol Biol* **13**, 238-252 (1965).
11. Jesorka, A. & Orwar, O. Liposomes: technologies and analytical applications. *Annu Rev Anal Chem* **1**, 801-832 (2008).
12. Bourgaux, C. & Couvreur, P. Interactions of anticancer drugs with biomembranes: what can we learn from model membranes? *J Control Release* **190**, 127-138 (2014).
13. Pinheiro, M., *et al.* The influence of rifabutin on human and bacterial membrane models: implications for its mechanism of action. *J Phys Chem B* **117**, 6187-6193 (2013).
14. Domenech, O., *et al.* Interactions of oritavancin, a new lipoglycopeptide derived from vancomycin, with phospholipid bilayers: Effect on membrane permeability and nanoscale lipid membrane organization. *Biochim Biophys Acta* **1788**, 1832-1840 (2009).
15. Haywood, A.M. & Boyer, B.P. Fusion of influenza virus membranes with liposomes at pH 7.5. *Proc Natl Acad Sci U S A* **82**, 4611-4615 (1985).
16. Weiss, V.U., *et al.* Liposomal leakage induced by virus-derived peptides, viral proteins, and entire virions: rapid analysis by chip electrophoresis. *Anal Chem* **82**, 8146-8152 (2010).
17. Weiss, V.U., Bilek, G., Pickl-Herk, A., Blaas, D. & Kenndler, E. Mimicking virus attachment to host cells employing liposomes: analysis by chip electrophoresis. *Electrophoresis* **30**, 2123-2128 (2009).
18. Fontana, J. & Steven, A.C. Influenza virus-mediated membrane fusion: Structural insights from electron microscopy. *Arch Biochem Biophys* **581**, 86-97 (2015).
19. Sapir, A., Avinoam, O., Podbilewicz, B. & Chernomordik, L.V. Viral and developmental cell fusion mechanisms: conservation and divergence. *Dev Cell* **14**, 11-21 (2008).
20. Marsh, M. & Helenius, A. Virus entry: open sesame. *Cell* **124**, 729-740 (2006).
21. Ono, A. & Freed, E.O. Plasma membrane rafts play a critical role in HIV-1 assembly and release. *Proc Natl Acad Sci U S A* **98**, 13925-13930 (2001).
22. Campbell, S.M., Crowe, S.M. & Mak, J. Virion-associated cholesterol is critical for the maintenance of HIV-1 structure and infectivity. *AIDS* **16**, 2253-2261 (2002).

23. Ohvo-Rekila, H., Ramstedt, B., Leppimaki, P. & Slotte, J.P. Cholesterol interactions with phospholipids in membranes. *Prog Lipid Res* **41**, 66-97 (2002).
24. Luscher-Mattli, M. Polyanions-a lost chance in the fight against HIV and other virus diseases? *Antivir Chem Chemother* **11**, 249-259 (2000).
25. Landazuri, N., Gupta, M. & Le Doux, J.M. Rapid concentration and purification of retrovirus by flocculation with Polybrene. *J Biotechnol* **125**, 529-539 (2006).
26. Ito, M., *et al.* Inhibitory effect of dextran sulfate and heparin on the replication of human immunodeficiency virus (HIV) in vitro. *Antiviral Res* **7**, 361-367 (1987).
27. Brugger, B., *et al.* The HIV lipidome: a raft with an unusual composition. *Proc Natl Acad Sci U S A* **103**, 2641-2646 (2006).
28. Dalgleish, A.G., *et al.* The CD4 (T4) antigen is an essential component of the receptor for the AIDS retrovirus. *Nature* **312**, 763-767 (1984).
29. Edidin, M. The state of lipid rafts: from model membranes to cells. *Annu Rev Biophys Biomol Struct* **32**, 257-283 (2003).
30. Kahveci, Z., Martinez-Tome, M.J., Esquembre, R., Mallavia, R. & Mateo, C.R. Selective Interaction of a Cationic Polyfluorene with Model Lipid Membranes: Anionic versus Zwitterionic Lipids. *Materials* **7**, 2120-2140 (2014).
31. Faudry, E., Perdu, C. & Attree, I. Pore formation by T3SS translocators: liposome leakage assay. *Methods Mol Biol* **966**, 173-185 (2013).
32. Coeytaux, E., Coulaud, D., Le Cam, E., Danos, O. & Kichler, A. The cationic amphipathic alpha-helix of HIV-1 viral protein R (Vpr) binds to nucleic acids, permeabilizes membranes, and efficiently transfects cells. *J Biol Chem* **278**, 18110-18116 (2003).
33. Kaplan, I.M., Wadia, J.S. & Dowdy, S.F. Cationic TAT peptide transduction domain enters cells by macropinocytosis. *J Control Release* **102**, 247-253 (2005).
34. White, J.M., Delos, S.E., Brecher, M. & Schornberg, K. Structures and mechanisms of viral membrane fusion proteins: multiple variations on a common theme. *Crit Rev Biochem Mol Biol* **43**, 189-219 (2008).